Published in final edited form as:
Chem Biol. 2010 August 27; 17(8): 892–902. doi:10.1016/j.chembiol.2010.06.006.

Modulation of Pantothenate Kinase 3 Activity by Small Molecules that Interact with the Substrate/Allosteric Regulatory Domain

Roberta Leonardi[1], **Yong-Mei Zhang**[1,4], **Mi-Kyung Yun**[2], **Ruobing Zhou**[1], **Fu-Yue Zeng**[3,5], **Wenwei Lin**[3], **Jimmy Cui**[3], **Taosheng Chen**[3], **Charles O. Rock**[1], **Stephen W. White**[2], and **Suzanne Jackowski**[1,*]

[1]Department of Infectious Diseases, St. Jude Children's Research Hospital, 262 Danny Thomas Place, Memphis, TN 38105

[2]Department of Structural Biology, St. Jude Children's Research Hospital, 262 Danny Thomas Place, Memphis, TN 38105

[3]Department of Chemical Biology and Therapeutics, St. Jude Children's Research Hospital, 262 Danny Thomas Place, Memphis, TN 38105

SUMMARY

Pantothenate kinase (PanK) catalyzes the rate-controlling step in coenzyme A (CoA) biosynthesis. PanK3 is stringently regulated by acetyl-CoA and uses an ordered kinetic mechanism with ATP as the leading substrate. Biochemical analysis of site-directed mutants indicates that pantothenate binds in a tunnel adjacent to the active site that is occupied by the pantothenate moiety of the acetyl-CoA regulator in the PanK3•acetyl-CoA binary complex. A high-throughput screen for PanK3 inhibitors and activators was applied to a bioactive compound library. Thiazolidinediones, sulfonylureas and steroids were inhibitors, and fatty acyl-amides and tamoxifen were activators. The PanK3 activators and inhibitors either stimulated or repressed CoA biosynthesis in HepG2/C3A cells. The flexible allosteric acetyl-CoA regulatory domain of PanK3 also binds the substrates, pantothenate and pantetheine, and small molecule inhibitors and activators to modulate PanK3 activity.

INTRODUCTION

Pantothenate kinases (PanK) are the regulatory enzymes that control the rate of CoA biosynthesis and the concentration of intracellular CoA (Leonardi et al., 2005b). In mammals, there are four characterized isoforms of PanK, PanK1α, PanK1β, PanK2 and PanK3, encoded by three genes. All four proteins share homologous catalytic core domains

*Correspondence: suzanne.jackowski@stjdue.org.
[4]Present address: Department of Biochemistry and Molecular Biology, Medical University of South Carolina, 173 Ashley Ave., Charleston, SC 29425
[5]Present address: Burnham Institute of Medical Research, 10901 North Torrey Pines Road, LaJolla, CA 92037

ACCESSION NUMBER

The coordinates for the PanK3•acetyl-CoA binary complex have been deposited in the Protein Data Bank with the accession number of 3MK6.

of approximately 350 amino acids. The enzymes function as homodimers with two equivalent active sites formed by a head-to-tail juxtaposition of the monomers. PanK3 and PanK1β contain only the catalytic core domain (Rock et al., 2002; Zhang et al., 2005), and PanK1α and PanK1β arise from the *PANK1* gene through the use of alternate initiation exons (Rock et al., 2002). PanK1α differs from PanK1β and PanK3 in having a ~230 residue amino terminal extension whose function is not understood. The *PANK2* gene encodes a protein that is processed twice during its localization to the mitochondria in humans (Hörtnagel et al., 2003), but mouse PanK2 lacks these signals and remains in the cytosol (Leonardi et al., 2007b). A common feature of mammalian PanKs is that they are regulated via feedback inhibition by acetyl-CoA (Leonardi et al., 2005b), which is the primary mechanism that controls kinase activity and the intracellular level of CoA (Rock et al., 2002; Zhang et al., 2005; Rock et al., 2003). PanKs bind acetyl-CoA with high affinity and the ligand remains bound to the enzymes through purification (Hong et al., 2007). Acyl-carnitines activate PanK2 by displacing acetyl-CoA from the enzyme (Leonardi et al., 2007a).

The discoveries that mutations in the *PANK2* gene are linked to pantothenate kinase-associated neurodegeneration (PKAN) (Zhou et al., 2001) and the connection between *PANK1* and insulin levels revealed in a recent genome-wide association study (Sabatti et al., 2009) have focused interest on understanding PanK. The first structure was the *Staphylococcus aureus* PanK (*Sa*PanK) complex with AMPPNP•Mg^{2+} (Hong et al., 2006). This structure, coupled with site-directed mutagenesis studies, revealed the residues important for nucleotide binding and catalysis; however, *Sa*PanK is not regulated by acetyl-CoA (Leonardi et al., 2005a). The acetyl-CoA binding site was revealed in structures of the PanK1β and PanK3 binary complexes with acetyl-CoA. The regulator docks in a linear pocket adjacent to the active site formed by residues derived from both monomers (Hong et al., 2007). The adenine portion of acetyl-CoA is not visible in these structures, but it was suggested that the ADP of CoA extends into the ATP binding cleft to block catalysis, thus explaining how acetyl-CoA inhibition is competitive with respect to ATP (Hong et al., 2007).

The understanding of PanK functions is limited by the dearth of information on the biochemistry of the PanKs. The structures of the PanK3 binary complexes do not reveal the binding pocket of the pantothenate substrate, but we did visualize the pantothenate in the structurally-related *Pseudomonas aeruginosa* PanK (*Pa*PanK). However, an equivalent pocket is absent in the mammalian PanKs due to distinct differences in their dimer interface compared to *Pa*PanK. Therefore, we hypothesized that pantothenate occupies the same pocket as the pantothenate moiety of acetyl-CoA (Hong et al., 2007). If correct, the extensive acetyl-CoA binding surface and the flexibility of the enclosing flap suggest that a biochemical screen would identify PanK inhibitors and activators with the potential to regulate intermediary metabolism in human diseases. PanK inhibitors would be used to explore the relationship between glucose homeostasis and hepatic CoA levels that were revealed by the treatment of animals with the pantothenate antimetabolite, hopantenate (Zhang et al., 2007) and by the analysis of PanK1 knockout mice (Leonardi et al., 2010). Activators, like furosemide, an activator of *Plasmodium falciparum* PanK (Lehane et al., 2007), could potentially increase CoA levels and alleviate the deficiency in CoA biosynthesis that arises from PanK2 inactivation in PKAN disease. PanK3 was selected to initiate this study because it is ubiquitously expressed and can be purified in the quantities necessary for structural analysis, site-directed mutagenesis and high-throughput screening (HTS).

RESULTS

Ordered Mechanism for PanK3

The kinetic parameters for ATP and pantothenate, and the kinetic mechanism for PanK3 were determined to provide the basis for the interpretation of the effects of mutations on enzyme activity and substrate binding. The K_M values for ATP and pantothenate were 311 ± 53 μM and 14 ± 0.1 μM, respectively. Product inhibition experiments showed that ADP was a competitive inhibitor of PanK3 with respect to ATP (Fig. 1A) and a mixed-type inhibitor with respect to pantothenate (Fig. 1B). These product inhibition data show that PanK3 operates via an ordered kinetic mechanism with ATP as the leading substrate (Fig. 1C). An ordered kinetic mechanism is common for kinases, and is also found in *E. coli* pantothenate kinase (Song and Jackowski, 1994), which has a completely different 3-dimensional structure than PanK3 and belongs to a different kinase family (Yun et al., 2000).

Structure-Guided Site-Directed Mutagenesis

As part of this study, we determined a higher resolution structure (Table 1) of the PanK3•acetyl-CoA complex than the one previously reported (Hong et al., 2007). The structures are very similar except that improved resolution revealed the location of the 3′,5′-AMP portion of acetyl-CoA that was previously not visible (Fig. 1D). The phosphate on the 3′-position of the ribose interacts with Lys24 and Arg325, and the 2′-hydroxyl group forms a hydrogen bond with the backbone amide of Gly116. The adenine ring is loosely held by interactions with Lys135 and Gly116, and Ile253′and Try254′ from the opposite monomer (Fig. 1D). We anticipated that the ATP-like moiety of acetyl-CoA would occupy the ATP binding site of PanK3, but comparison with the *Sa*PanK•ATP•Mg^{2+} binary complex structure (Hong et al., 2006) shows that this is not the case. The modes of binding are similar, but the adenine ring of acetyl-CoA engages a different site at the interface of the two subdomains. In the *Sa*PanK•ATP•Mg^{2+} binary complex, these two domains are in a closed conformation that is required for catalysis (Hong et al., 2006), but the adenine portion of acetyl-CoA sits in the ATP binding cleft, holding it in an open conformation that does not allow ATP to enter the active site and engage the P-loop.

The site-directed mutagenesis strategy was to identify a side chain modification in the pantothenate-binding portion of the acetyl-CoA tunnel that renders PanK3 refractory to acetyl-CoA inhibition. The contacts between acetyl-CoA and PanK3 are similar to those responsible for the β-strand interactions within the β-sheet of a protein (Fig. 1D). The α7′-β13′loop reaches over from the opposite subunit to form the ‘lid’ of the tunnel, and only interacts with acetyl-CoA via the backbone carbonyls of Ala269′ and Val268′ and the amide nitrogens of 4′-phosphopantetheine. These interactions cannot be altered by amino acid replacements. However, Ser195 and Arg207 on strands β10 and β11, respectively, have side-chain interactions with acetyl-CoA (Fig. 1D). The side chain of Ser195 extends into the tunnel to form a hydrogen bond with the pantothenate carbonyl oxygen, and we mutated this residue to a valine to introduce a bulkier side chain that could compromise the docking of ligands within the tunnel by steric hindrance. The guanidinium group of Arg207 has a strong interaction with the carbonyl oxygen of the β-alanine segment of the 4′-phosphopantetheine (Fig. 1D), and we hypothesized that an equivalent interaction with the terminal carboxyl group of pantothenate would serve to register the substrate within the tunnel. Arg207 was therefore changed to an alanine to eliminate this potential interaction. Finally, alanines 267′ and 269′ mediate tight van der Waals interactions with the pantothenate moiety. Ala267 contacts the mercaptoethanolamine group and Ala269 interacts with the methyl groups (Fig. 1D). Both were mutated to Phe to sterically interfere with ligand binding.

The PanK3(R207A), PanK3(A267F) and PanK3(A269F) mutants were all catalytically inactive (<1% wild-type activity under all conditions tested) despite being correctly folded based on their Stoke's radius determined by gel filtration chromatography (not shown). Furthermore, the proteins bound ATP normally based on the Kd's for the binding of the fluorescent ATP analog TNP-ATP (see Supplementary Experimental Procedures). PanK3 exhibited an apparent Kd for TNP-ATP of 3.6 ± 0.9 μM, and the values determined for PanK3(R207A) (3.0 ±0.3 μM), PanK3(A267F) (3.1 ± 0.8 μM), and PanK3(A269F) (5.4 ± 0.8 μM) indicated that the inactive mutant enzymes were not defective in ATP binding. These data supported the idea that the allosteric domain of the protein involved in the binding of the 4′-phosphopantetheine portion of acetyl-CoA was also critical for either pantothenate binding or catalysis.

PanK3(S195V) was the most informative mutant. PanK3(S195V) was a catalytically active protein that retained 30% of the wild-type specific activity under our standard assay condition but was refractory to inhibition by acetyl-CoA (Fig. 1E), illustrating that the introduction of the bulky valine group into the tunnel prevented the binding of acetyl-CoA. The kinetic analysis of PanK3(S195V) showed an ATP K_M = 191 ± 27 μM compared to 311 ± 53 for PanK3, but PanK3(S195V) exhibited a 10-fold increase in the K_M for pantothenate (151 ± 16 μM) compared to PanK3 (14 ± 0.1) ($p<0.01$). The simultaneous perturbation of both pantothenate and acetyl-CoA binding in the PanK3(S195V) mutant provided strong support for the idea that the two ligands share a common binding site on the protein.

Utilization of Pantetheine by PanK3

If pantothenate binds at approximately the same location as the longer pantetheine portion of acetyl-CoA, then substrate analogs that extend from the carboxyl end of pantothenate would be anticipated to also be substrates. PanK3 phosphorylates hopantenate, a pantothenate analog that is 1-carbon longer than pantothenate (Zhang et al., 2007), and it is also able to phosphorylate the N-pentyl- and N-heptyl-pantothenamide analogs of pantothenate that have different alkyl extensions linked to the carboxyl group (Virga et al., 2006). These data illustrate that extensions of pantothenate from the carboxyl end of the molecule are readily tolerated by PanK. Thus, pantetheine is a likely substrate for PanK3, although the physiological significance of this reaction is unclear. PanK3 readily phosphorylated pantetheine with an apparent K_M of 23 ± 2 μM. The K_M of PanK3(S195V) for pantetheine (59 ± 3 μM) was higher than for PanK ($p<0.01$). These findings corroborate the conclusion that the pantothenate/pantetheine substrate binding site was compromised in PanK3(S195V).

Bioactive Compound Library Screen

A biochemical high-throughput screen (HTS) was developed to identify small molecule inhibitors and activators of PanK3 using a two-step luminescence-based assay similar to the assay employed to screen other kinases, like *Mycobacterium tuberculosis* pantothenate kinase (Habig et al., 2009). In the first step, PanK3 was incubated with the substrates and the test compound, and in the second step, a mixture of luciferase and luciferin was added and the luminescence measured. The measured signal was proportional to the amount of ATP remaining after the PanK3 reaction, so that activators and inhibitors produced either a low or high signal, respectively, compared to the DMSO control. To enable the detection of both activators and inhibitors, the substrate concentrations, amount of PanK3 and incubation time were adjusted so that ~35% of ATP was consumed in control reactions. The reactions were started by the addition of PanK3, which was stable at 4°C for ≥24 h. One caveat to this screen is that it would not detect PanK competitive inhibitors that are also substrates if their affinities for PanK were similar to pantothenate (Spry et al., 2010).

The PanK3 HTS assay was used to screen a compound collection containing 5,600 (3,200 unique) molecules with known biological activity. All compounds were initially screened at 12 μM, and the Z′ parameter was used to assess assay performance (Zhang et al., 1999). Z′ was consistent throughout the screen with an average value >0.5, illustrating that the assay was stable and reproducible from plate to plate (Supplementary Figs. S1A-S1C). We also did not observe any plate well positional trends based on the average activities of each well in all plates screened (data not shown). A summary of the entire data set calculated to identify both inhibitors and activators is shown in Supplementary Figs. S1D & S1F. Cut-off values of >25% activation and >30% inhibition of PanK3 identified 8 unique activators (13 total) and 44 unique inhibitors (65 total). A 10-point dose-response curve in triplicate was subsequently obtained to validate each of the primary hits using the HTS platform (Supplementary Figs. S1E & S1G). This validation step led to the exclusion of 6 inhibitors (13.6%) and 1 activator (12.5%) as false positives.

PanK3 Inhibitors from the HTS

The HTS identified and confirmed 20 inhibitors of PanK3 with an IC_{50} <10 μM (Table 2). We focused our mechanistic analyses on three classes of inhibitors, thiazolidinediones, sulfonylureas, and steroids, which had multiple hits in the HTS. The two thiazolidinediones detected in the screen were rosiglitazone and pioglitazone (Table 2). This class of compounds are best known as PPARγ ligands that are widely used for the treatment of type 2 diabetes (Gale, 2001;Lehmann et al., 1995;Mudaliar and Henry, 2001). The two sulfonylurea inhibitors identified in the assay, glipizide and glyburide (Table 2), are second generation sulfonylureas that stimulate insulin secretion from the pancreatic β-cells and are widely prescribed oral antidiabetic drugs (Bell, 2004;Boyd et al., 1990). The most potent inhibitor was fusidic acid, one of three steroid-like compounds that were identified in the screen (Table 2). Fusidic acid is an antibiotic effective against methicillin-resistant *S. aureus* and other Gram-positive bacteria, but it is not extensively used due to hepatotoxic side effects (Bode et al., 2002;Humble et al., 1980). The two other steroid-like inhibitors, pregnenolone sulfate and dehydroisoandrosterone sulfate, are synthesized in the brain and act as modulators of neurotransmitter receptors (Gibbs et al., 2006;Vallee et al., 2001). Additional representative members of each of the three structural classes were analyzed further to validate the HTS, derive initial structure-activity relationship (SAR) information and provide insights into their mechanism of action (Fig. 2).

Fusidic acid had an IC_{50} of 0.1 μM in the HTS assay (Table 2). Analogs of this structurally complex, steroid-like natural product (Fig. 2A) were not available, so we focused on investigating the SAR in a series of steroids related to the two identified in the HTS (Table 2). Sulfated steroids and their non-sulfated counterparts (Fig. 2A) were tested as PanK3 inhibitors using the radiochemical assay at a concentration of 100 μM (Fig. 3A). With the exception of estradiol sulfate, which had no effect on PanK3, pregnenolone, dehydroisoandrosterone and estrone sulfates inhibited the enzyme more potently than their non-sulfated versions. Conversion of dehydroisoandrosterone sulfate to estrone sulfate through aromatization of the A ring of the sterane core reduced inhibitor activity. Pregnenolone and cholesterol have different substituents replacing the ketone at C17, and these compounds were weak PanK3 inhibitors, highlighting the importance of this functional group at C17. Dehydroisoandrosterone decreased the enzyme activity even in the absence of the sulfate group at C-3. This SAR information revealed that, in addition to the sulfate group on the C-3, a keto or methyl keto group on C-17 was also important for inhibiting PanK3. Although these data validated the HTS approach and revealed a clear SAR among the steroids tested, their weak potency and chemical properties make them undesirable scaffolds to develop as selective biological modifiers, and their mechanism of action was not investigated further.

The thiazolidinediones and sulfonylureas are used in the treatment of type 2 diabetes. The thiazolidinediones identified in the HTS and two additional members of this compound class not present in the library, ciglitazone and MCC-555 (Fig. 2B), have similar potencies as PanK3 inhibitors (Fig. 3B). MCC-555 was the most potent of the compounds with an IC_{50} of 5 μM (Fig. 3B). The potent PPARγ ligands, GW9662 and GW1929, either had no effect or very weak activity against PanK3 (Fig. 3B), illustrating that PPARγ activity can be separated from PanK activity. GW501516, a PPARδ selective ligand (Sznaidman et al., 2003) that has a related thiazole ring instead of a thiazolidinedione ring (Fig. 2B), showed weak activity against PanK3 (IC_{50} ~100 μM). The sulfonylureas, glyburide and glipizide (Fig. 2C), were confirmed as PanK3 inhibitors (IC_{50} = 8.5 μM) by the radioactive assay (Fig. 3C). Tolbutamide, a first generation sulfonylurea, was ineffective against the enzyme. The non-sulfonylurea insulin secretagogues, nateglinide and repaglinade (Fig. 2C) were also inactive (IC_{50} > 100μM) (Fig. 3C). These data showed that, among insulin secretagogues, only the sulonylurea series were PanK inhibitors.

Thiazolidinediones and Sulfonylureas Target the Acetyl-CoA Binding Site

Our structure of the PanK3•acetyl-CoA binary complex showed that the adenine moiety of acetyl-CoA docks into the cleft that binds ATP, prevents ATP binding and maintains the enzyme in an ‘open’ conformation (Fig. 1D). To test whether any of the thiazolidindiones and sulfonylureas bind to the regulatory acetyl-CoA binding site, a representative member of each group (MCC-555 and glyburide) was tested for their ability to inhibit PanK3(S195V) and *S. aureus* PanK (*Sa*PanK). PanK3(S195V) is refractory to feed-back inhibition by acetyl-CoA (Fig. 1E), and *Sa*PanK is a bacterial PanK with the same structural fold as PanK3, but is not allosterically regulated by acetyl-CoA (Leonardi et al., 2005a). A comparison between the structures of the PanK3•acetyl-CoA (Fig. 2A) and *Sa*PanK•AMP-PNP•Mg^{2+} complexes (Hong et al., 2006) suggested that acetyl-CoA binding to *Sa*PanK may be prevented in part by the side chains of Tyr240 and Arg244 that substitute for Ala337 and Trp341, respectively, in PanK3 (Hong et al., 2007). We also note that the loop in *Sa*PanK corresponding to the α7′-β13′loop in PanK3 that forms the ‘lid’ of the active site tunnel is disordered in *Sa*PanK•AMP-PNP•Mg^{2+}, consistent with this crystal structure representing the empty ‘open’ configuration of the pantothenate binding site. PanK3(S195V) and *Sa*Pank were both refractory to MCC-555 and glyburide inhibition (Fig. 3D and 3E), suggesting that the binding site for these two inhibitors overlaps with the pantothenate/acetyl-CoA site within the substrate binding tunnel. The kinetic mechanism underlying PanK3 inhibition by MCC-555 and glyburide was also investigated, and they both were uncompetitive with respect to ATP and pantothenate (Supplementary Fig. S2). Based on the compulsory ordered kinetic mechanism of PanK3 (Fig. 1C), this kinetic analysis indicates that both compounds bind to the PanK3•ADP complex (Supplementary Fig. S2E). Thus, the thiazolidinedione and sulfonylureas appear to interact in the vicinity of the acetyl-CoA regulatory site to inhibit PanK3 activity, but may not extend into the ATP binding cleft to prevent binding of the nucleotide.

Identification of PanK3 Activators

PanK3 activators validated by HTS and with an EC_{50} <10 μM are listed in Table 3. These compounds were further tested using the radioactive PanK assay, and 1,4-napthoquinone and phenylmercuric acid were not confirmed as PanK3 modulators. The HTS assay relied on the signal produced by the luciferase reaction and a compound that dose-dependently inhibited this step would therefore appear as an activator in this assay, but not in the radiochemical assay. Thus, the HTS assay only identified two *bona fide* activators, and produced a higher rate of false positive hits compared to the inhibitor hits.

Oleoyl-ethanolamide was one of the confirmed activators (Fig. 2D and Table 3). This PPARα ligand (Hansen and Diep, 2009;Schwartz et al., 2008) belongs to a class of phosphatidylethanolamine-derived metabolites referred to as endocannabinoids, and it activated PanK3 with the same potency as palmitoylcarnitine, a known activator of both PanK2 (Leonardi et al., 2007a) and PanK3 (Table 3). This hit in the HTS was further explored by using the radioactive assay to screen the Enzo endocannabinoid library, a collection of 60 compounds representing the combination of 10 acyl chains attached to 6 different amines (Supplementary Table S1). These compounds were tested at 1 and 10 μM for their ability to relieve PanK3 inhibition by acetyl-CoA using the radiochemical assay. The endocannabinoid library screen was performed in the presence of acetyl-CoA because palmitoyl-carnitine activates PanK2 by competing with the allosteric inhibitor, acetyl-CoA (Leonardi et al., 2007a), and we were interested in evaluating the effectiveness of potential activators to reverse acetyl-CoA inhibition. Within the same class of compounds, an 18:1 acyl chain activated PanK3 more potently than 16:0 (Supplementary Table S1), reflecting the higher potency of oleoyl-carnitine compared to palmitoyl-carnitine as a PanK3 activator (Table 3). The screen revealed that acyl-glycines and acyl-GABAs were more potent than the acyl-amides, -ethanolamides, -alanines and –dopamines, but oleoyl-glycine and oleoyl-GABA were not more potent activators than oleoyl-carnitine (Table 3 and Supplementary Table S1). We previously reported that PanK2 activation by palmitoyl-carnitine was competitive with respect to acetyl-CoA, and this regulatory event functions to increase the CoA levels to support β-oxidation (Leonardi et al., 2007a). Competition between acetyl-CoA and oleoyl-carnitine was also observed with PanK3 (data not shown), and illustrates that PanK2 and PanK3 are regulated in a similar manner by acyl-carnitines. However, these lipophilic activators are not suitable chemical scaffolds for developing small molecule activators due to their hydrophobicity and metabolic instability. Tamoxifen is an estrogen receptor antagonist and was the second confirmed activator of PanK3 with an EC_{50} of 4 μM (Table 3). Like the acyl-carnitines, tamoxifen reversed the inhibition of PanK3 by acetyl-CoA (not shown) indicating that it activates PanK3 by inhibiting the binding of acetyl-CoA. Thus, tamoxifen activates PanK3 in a similar fashion to the activation of *Plasmodium falciparum* PanK by furosemide (Lehane et al., 2007), a drug that was present in two instances in our bioactive library that did not make the cutoff for an activator of PanK3.

Modulation of CoA Biosynthesis in HepG2/C3A Cells

We used HepG2/C3A cells to test the effect of inhibitors and activators on CoA biosynthesis in a human liver cell line. RT-PCR quantification of the PanK transcripts revealed that PanK3 was the most abundant isoform (Fig. 4A), thus making C3A cells a good model system to test the ability of representatives from each chemical class identified in the screen to modulate CoA biosynthesis in intact cells. The thiazolidinediones, MCC-555 and rosiglitazone, inhibited pantothenate incorporation into CoA in C3A cells (Fig. 4B). MCC-555 was a more potent CoA biosynthesis inhibitor than rosiglitazone in this assay, correlating with the biochemical assay (Fig. 3A). Glyburide also inhibited cellular CoA biosynthesis to a lesser extent than MCC-555 (Fig. 4B). Oleoyl-carnitine and oleoyl-ethanolamide were activators of CoA biosynthesis in C3A cells (Fig. 4B), but were less potent in cells than in vitro, likely due to the metabolism of the intermediates by the cells. Tamoxifen was the most potent activator of CoA biosynthesis in cells (Fig. 4B), reflecting the in vitro activity of the compound (Table 3). These data showed that PanK3 modulators identified in the screen modulated CoA biosynthesis in intact cells. Although the PanK modulators altered CoA synthesis in cell models, none of the compounds identified in the bioactive screen are suitable experimental tools to investigate PanK function due to their documented, higher affinitiy effects on other protein targets.

Isoform Selectivity

PanK1β and PanK2 were purified and their responses to MCC-555, glyburide and tamoxifen were compared to their effect on PanK3 (Supplementary Fig. S3). MCC-555 inhibited all three isoforms with a rank order of PanK3>PanK2>PanK1β. PanK2 was less sensitive to glyburide than PanK3, but PanK1β was activated rather than inhibited by this compound. In the case of tamoxifen, PanK2 was not affected by this drug and PanK1β was inhibited. A comparison of the CoA binding pockets of PanK3 and PanK1β (Hong et al., 2007) reveals that Trp266′ is replaced by Ser266′ and Tyr340 is replaced by Phe340, respectively. It is tempting to suggest that these differences account for the differential effect on the highly related PanK isoforms, but this interpretation is likely too simplistic. The loop that forms the lid of the tunnel is very flexible and may assume different conformations depending on the structure of the bound ligand that is sandwiched between the loop and the platform formed by strands β10–β11. These data indicate that PanK1β inhibitors can be obtained from an HTS screen using PanK3, and that there are sufficient differences between the structures of the PanKs that isoform-selective compounds can also be identified.

DISCUSSION

An important advance in the understanding of the PanK catalysis and regulation is the concept that the pantothenate substrate binding site overlaps with the docking site for the allosteric regulator, acetyl-CoA. A comparison between the PanK3•acetyl-CoA and *Sa*PanK•ATP•Mg^{2+} structures reveals that the former is locked in an ‘open’ conformation by acetyl-CoA. This comparison allowed a model of the PanK3•pantothenate•ATP•Mg^{2+} ‘closed’ ternary complex to be generated from the *Sa*PanK structure (Fig. 5). This model illustrates that pantothenate binding at the same location as the pantothenate portion of acetyl-CoA is consistent with the positioning of the catalytic base, Glu138, and the γ-phosphate of ATP in a complex poised for phosphoryl transfer (Fig. 5). The pantothenate binding site is formed by strands β10 and β11 on the monomer binding ATP•Mg^{2+} and the flexible α7′-β13′ loop from the opposite monomer. The analogous region in the *Sa*PanK•AMP-PNP•Mg^{2+} binary complex is disordered in the structure (Hong et al., 2006), which suggests that the α7′-β13′ substrate binding loop is disordered in the absence of either acetyl-CoA or pantothenate. Indeed, the pantothenate portion of acetyl-CoA cannot insert into the tight tunnel adjacent to the active site unless the α7′-β13′ ‘lid’ moves away from the β10–β11 strands that form the ‘floor’ of the tunnel (Figs. 1D). The structural alignment between the two proteins shows that the Ser102/Arg113 pair of *Sa*PanK is analogous to Ser195/Arg207 of PanK3 consistent with these residues playing a role in binding and orienting the pantothenate substrate at the active site.

The comparison between *Sa*PanK and PanK3 structures indicates that the substrate and regulator binding domain formed by the interaction between the monomers is not a static structure. We propose pantothenate first binds to the Ser195/Arg207 docking site on the rigid β10–β11 ‘floor’ on the subunit containing bound ATP•Mg^{2+}, followed by the flexible α7′-β13′ loop on the opposite monomer closing over the substrate to form a pantothenate-binding tunnel adjacent to the active site that aligns the 4′-hydroxyl for attack on the γ-phosphate of ATP catalyzed by the general base, Glu138. Direct evidence for this binding mode for pantothenate comes from the analysis of the PanK3(S195V) mutant, which is refractory to acetyl-CoA inhibition and has a lower affinity for pantothenate and pantetheine substrates. PanK3 also uses pantothenamides with alkyl chains up to 7 carbons in length as substrates (Virga et al., 2006), consistent with the substrate binding pocket in mammalian PanKs being able to accommodate extended pantothenate analogs. Finally, the PanK3(R207A), PanK3(A267F) and PanK3(A269F) mutants bind ATP normally but are catalytically inactive, supporting the conclusion that the tunnel architecture is important not only for binding the allosteric inhibitor but also for binding the pantothenate substrate. One

caveat to this conclusion is that pantothenate binds at a different location in the *Pa*PanK enzyme (Hong et al., 2006). Although *Pa*PanK is structurally related to PanK3 and *Sa*PanK, the radically different dimeric architecture of *Pa*PanK probably accounts for the unique positioning of pantothenate in the *Pa*PanK-pantothenate binary complex (Hong et al., 2006). Unlike PanK3 and *Sa*PanK, *Pa*PanK does not utilize the pantothenamide analogs as substrates (Hong et al., 2006), illustrating that the substrate binding pocket of *Pa*PanK is different from the other pantothenate kinases.

This study identified two chemical scaffolds in the bioactive compound library that bind to the acetyl-CoA regulatory site on PanK3 and inhibit the enzyme. Interestingly, both the thiazolidinediones and sulfonylureas identified in the primary screen (Table 2) are used in the treatment of type 2 diabetes (Gale, 2001;Lehmann et al., 1995;Mudaliar and Henry, 2001;Bell, 2004;Boyd et al., 1990). The affinity of rosiglitazone for PanK3 is comparable to the affinity of this thiazolidinedione for the free fatty acid receptor (Smith et al., 2009), another of its identified cellular targets. The SAR analysis shows that the highest activity PPARγ ligands or insulin secretagogues are not recognized by PanK3. At the other end of the spectrum, MCC-555 has a 50-fold lower affinity for PPARγ compared to rosiglitizone (Reginato et al., 1998), and the comparable potency of this compound toward PanK3 suggests that PanK3 should be given consideration as an off-target site of action. This is particularly interesting in light of the importance of CoA in supporting β-oxidation and gluconeogenesis. Hopantenate, a competitive inhibitor of PanK, reduces hepatic CoA levels leading to the accumulation of triglycerides and hypoglycemia, which is exacerbated by fasting (Zhang et al., 2007). Two phenotypes of the *Pank1* knockout mouse are lower serum triglycerides and glucose (Leonardi et al., 2010), suggesting that the pharmacological manipulation of CoA levels by PanK inhibitors may be potentially useful in the management of metabolic disorders. Also, the genome-wide association of polymorphisms in the *PANK1* gene with insulin levels (Sabatti et al., 2009) shows that PanK activity is associated with glucose homeostasis. These findings indicate that PanK regulation of CoA biosynthesis plays a key role in glucose homeostasis and fatty acid metabolism in liver. The robust PanK HTS is poised to be deployed to screen larger compound libraries to identify novel small molecules that are suitable for development as general and isoform-selective PanK modulators to probe the role of PanK in cell physiology and potentially to pharmacologically adjust imbalances in intermediary metabolism.

SIGNIFICANCE

The pantothenate kinases are a conserved group of proteins that regulate the synthesis of CoA, a key cellular cofactor in intermediary metabolism. The primary mechanism for PanK regulation is feedback inhibition by acetyl-CoA, and the discovery that this allosteric regulator docks to the pantothenate substrate site to block ATP binding provides a molecular explanation for the stringency of PanK regulation. The acetyl-CoA/pantothenate binding site consists of an extensive surface formed by a rigid platform on the monomer which binds ATP that engages a flexible segment from the opposite monomer to sandwich either the substrate or the allosteric regulator between the two monomers. This interaction surface provides a binding site for small molecules. PanK inhibitors and activators would be useful tools to establish the role of the PanKs in metabolism and disease. The importance of CoA levels in supporting gluconeogenesis and fatty acid oxidation is evident from the effects of CoA depletion in mice using the competitive PanK inhibitor hopantenate and the analysis of PanK1 knockout mice. Because PanK inhibition alters glucose and lipid homeostasis, the cross-reactivity of the thiazolidinedione and sulfonylurea scaffolds with PanK3 suggests that PanK activity should be tested for a potential off-target effect when considering the specificity of newly developed compounds. There are two established roles for PanK in human disease. Mutations in the *PANK2* gene give rise to the neurodegenerative disorder

known as PKAN, and a genome-wide association study linked polymorphisms in the *PANK1* gene to insulin levels. This study shows that small molecule PanK modulators can be identified and used to determine the importance of regulating the intracellular CoA levels in intermediary metabolism and disease.

EXPERIMENTAL PROCEDURES

Materials

Oligonucleotides were from the Hartwell Center at the St. Jude Children's Research Hospital; D-[1-^{14}C]pantothenate (specific activity, 55 mCi/mmol) was from American Radiolabeled Chemicals; TNP-ATP was from Molecular Probes, Invitrogen; Kinase Glo Plus luminescent kinase assay was from Promega; the endocannabinoid library was from Enzo Life Sciences; DMEM powder medium lacking glucose, sodium pyruvate, pantothenate and glutamine was from Gibco. Pantetheine was prepared by incubating pantetheine (1.4 mmoles) in 6 ml of 50 mM Tris-HCl, pH 8.0, 1 M DTT for 1 h at 60°C. All other reagents were of analytical grade or better.

Purification, Assay and Kinetics of PanK3

PanK3 was mutagenized using the QuickChange site-directed mutagenesis kit (Stratagene), as per manufacturer's instructions. Wild-type and mutant PanK3 proteins were purified by affinity chromatography and gel filtration to homogeneity as described (Hong et al., 2007) by the St. Jude Protein Production Facility. Enzymatic activity was determined in mixtures containing 45 μM D-[1-^{14}C]pantothenate (specific activity 22.5 mCi/mmol), 250 μM ATP, 10 mM $MgCl_2$, 0.1 M Tris-HCl pH 7.5, and increasing amounts of protein from 50 ng to 1.6 μg. The K_M for pantothenate was determined in reaction mixtures containing 2 to 180 μM of this substrate and 10 mM ATP. The K_M for ATP was determined in reaction mixtures containing 45 μM of pantothenate and increasing ATP concentrations from 4 μM to 1 mM. The same experiments were repeated in the presence of 0, 200 and 625 μM ADP to elucidate the kinetic mechanism. The potency of activators and inhibitors was evaluated in standard mixtures containing 250 μM ATP, increasing concentrations of the compound, and either 200 ng of PanK3, 10 ng of *Sa*PanK or 800 ng of PanK3(S195V). Compounds of the endocannabinoid library were tested in reactions containing 1.2 μM acetyl-CoA and 1 or 10 μM of each test compounds. All reactions were incubated at 37°C for 10 minutes, then stopped by the addition of 4 μl of 10% acetic acid. A 40 μl aliquot was deposited onto a Whatmann DE81 ion-exchange filter disk that was washed in three changes of 1% acetic acid/95% ethanol. Radioactive 4′-phosphopantothenate was quantified by counting each dried disk in 3 ml of scintillation fluid.

High-Throughput Screening (HTS)

The PanK3 HTS was performed using the St. Jude Children's Research Hospital (Memphis, TN USA) bioactive compound library consisting of 5,600 (3,200 unique) bioactive molecules. The sources were: 1,280 compounds from Sigma (Cat #LO1280), 3,200 compounds from Microsource (Gaylordsville, CT; the "Spectrum Collection", the "US Drug Collection", and the "Killer plates"), and 1,120 compounds from Prestwick (Illkirch, France; the "Prestwick Chemical Library"). The HTS assay is detailed in Supplementary Experimental Procedures.

CoA Biosynthesis in HepG2/C3A Cells

HepG2/C3A cells were cultured in EMEM medium supplemented with 10% fetal bovine serum and 2 mM glutamine, 50 U/ml penicillin and 50 μg/ml streptomycin. Labeling medium was prepared from glucose-, pantothenate-, pyruvate- and glutamine-free DMEM

medium reconstituted with 1 g/l glucose, 1 mM pyruvate, 2 mM glutamine, 1 μCi/ml [2,3-^{3}H]pantothenic acid (specific activity 50 Ci/mmol), and containing 4 mM octanoate, 5% dialyzed FBS, 50 U/ml penicillin and 50 μg/ml streptomycin. Cells were seeded at a density of 2–3 × 10^6 in 60-mm dishes and allowed to adhere overnight. The labeling was initiated by replacing the medium with 2 ml of labeling medium containing DMSO (control) or the test compound. Cells were incubated for 24 h, the labeling medium was removed, cells were washed with phosphate-buffered saline and lysed by the addition of 200 μl of 25% formic acid containing 50 mM DTT. The lysates (80 μl) were deposited onto a Whatman DE81 filter disk that was washed with three changes of 1% acetic acid/95% ethanol. [^{3}H]Phosphorylated metabolites were quantified by counting the dried disks. The assay measures all intermediates downstream of pantothenate; however, >98% of all of the radiolabled metabolites are CoA based on chromatographic analysis (Zhang et al., 2007).

Supplementary Material

Refer to Web version on PubMed Central for supplementary material.

Acknowledgments

We thank Karen Miller and Matt Frank for their expert technical assistance, and Richard Heath and the St. Jude Protein Production Facility for protein preparation. This work was supported by National Institutes of Health grant GM 062896, Cancer Center (CORE) Support Grant CA21765 and the American Lebanese Syrian Associated Charities.

REFERENCES

Bell DS. Practical considerations and guidelines for dosing sulfonylureas as monotherapy or combination therapy. Clin. Ther. 2004; 26:1714–1727. [PubMed: 15639686]

Bode KA, Donner MG, Leier I, Keppler D. Inhibition of transport across the hepatocyte canalicular membrane by the antibiotic fusidate. Biochem. Pharmacol. 2002; 64:151–158. [PubMed: 12106615]

Boyd AE, Aguilar-Bryan L, Nelson DA. Molecular mechanisms of action of glyburide on the beta cell. Am. J. Med. 1990; 89:3S–10S. [PubMed: 2117388]

Gale EA. Lessons from the glitazones: a story of drug development. Lancet. 2001; 357:1870–1875. [PubMed: 11410214]

Gibbs TT, Russek SJ, Farb DH. Sulfated steroids as endogenous neuromodulators. Pharmacol. Biochem. Behav. 2006; 84:555–567. [PubMed: 17023038]

Habig M, Blechschmidt A, Dressler S, Hess B, Patel V, Billich A, Ostermeier C, Beer D, Klumpp M. Efficient elimination of nonstoichiometric enzyme inhibitors from HTS hit lists. J. Biomol. Screen. 2009; 14:679–689. [PubMed: 19470716]

Hansen HS, Diep TA. N-acylethanolamines, anandamide and food intake. Biochem. Pharmacol. 2009; 78:553–560. [PubMed: 19413995]

Hong BS, Senisterra G, Rabeh WM, Vedadi M, Leonardi R, Zhang YM, Rock CO, Jackowski S, Park HW. Crystal structures of human pantothenate kinases. Insights into allosteric regulation and mutations linked to a neurodegeneration disorder. J. Biol. Chem. 2007; 282:27984–27993. [PubMed: 17631502]

Hong BS, Yun MK, Zhang Y-M, Chohnan S, Rock CO, White SW, Jackowski S, Park HW, Leonardi R. Prokaryotic type II and type III pantothenate kinases: The same monomer fold creates dimers with distinct catalytic properties. Structure. 2006; 14:1251–1261. [PubMed: 16905099]

Hörtnagel K, Prokisch H, Meitinger T. An isoform of hPANK2, deficient in pantothenate kinase-associated neurodegeneration, localizes to mitochondria. Hum. Mol. Genet. 2003; 12:321–327. [PubMed: 12554685]

Humble MW, Eykyn S, Phillips I. Staphylococcal bacteraemia, fusidic acid, and jaundice. Br. Med. J. 1980; 280:1495–1498. [PubMed: 7388562]

Lehane AM, Marchetti RV, Spry C, van Schalkwyk DA, Teng R, Kirk K, Saliba KJ. Feedback inhibition of pantothenate kinase regulates pantothenol uptake by the malaria parasite. J. Biol. Chem. 2007; 282:25395–25405. [PubMed: 17581817]

Lehmann JM, Moore LB, Smith-Oliver TA, Wilkison WO, Willson TM, Kliewer SA. An antidiabetic thiazolidinedione is a high affinity ligand for peroxisome proliferatoractivated receptor gamma (PPAR gamma). J. Biol. Chem. 1995; 270:12953–12956. [PubMed: 7768881]

Leonardi R, Chohnan S, Zhang Y-M, Virga KG, Lee RE, Rock CO, Jackowski S. A pantothenate kinase from Staphylococcus aureus refractory to feedback regulation by coenzyme A. J. Biol. Chem. 2005a; 280:3314–3322. [PubMed: 15548531]

Leonardi R, Rehg JE, Rock CO, Jackowski S. Pantothenate kinase 1 is required to support the metabolic transition from the fed to the fasted state. PLoS ONE. 2010 *(in press)*.

Leonardi R, Rock CO, Jackowski S, Zhang Y-M. Activation of human mitochondrial pantothenate kinase 2 by palmitoylcarnitine. Proc. Natl. Acad. Sci. U. S. A. 2007a; 104:1494–1499. [PubMed: 17242360]

Leonardi R, Zhang YM, Lykidis A, Rock CO, Jackowski S. Localization and regulation of mouse pantothenate kinase 2. FEBS Lett. 2007b; 581:4639–4644. [PubMed: 17825826]

Leonardi R, Zhang Y-M, Rock CO, Jackowski S. Coenzyme A: Back in action. Prog. Lipid Res. 2005b; 44:125–153. [PubMed: 15893380]

Mudaliar S, Henry RR. New oral therapies for type 2 diabetes mellitus: The glitazones or insulin sensitizers. Annu. Rev. Med. 2001; 52:239–257. [PubMed: 11160777]

Reginato MJ, Bailey ST, Krakow SL, Minami C, Ishii S, Tanaka H, Lazar MA. A potent antidiabetic thiazolidinedione with unique peroxisome proliferator-activated receptor γ-activating properties. J. Biol. Chem. 1998; 273:32679–32684. [PubMed: 9830009]

Rock CO, Karim MA, Zhang Y-M, Jackowski S. The murine *Pank1* gene encodes two differentially regulated pantothenate kinase isozymes. Gene. 2002; 291:35–43. [PubMed: 12095677]

Rock CO, Park H-W, Jackowski S. Role of feedback regulation of pantothenate kinase (CoaA) in the control of coenzyme A levels in *Escherichia coli*. J. Bacteriol. 2003; 185:3410–3415. [PubMed: 12754240]

Sabatti C, Service SK, Hartikainen AL, Pouta A, Ripatti S, Brodsky J, Jones CG, Zaitlen NA, Varilo T, Kaakinen M, et al. Genome-wide association analysis of metabolic traits in a birth cohort from a founder population. Nat. Genet. 2009; 41:35–46. [PubMed: 19060910]

Schwartz GJ, Fu J, Astarita G, Li X, Gaetani S, Campolongo P, Cuomo V, Piomelli D. The lipid messenger OEA links dietary fat intake to satiety. Cell Metab. 2008; 8:281–288. [PubMed: 18840358]

Smith NJ, Stoddart LA, Devine NM, Jenkins L, Milligan G. The action and mode of binding of thiazolidinedione ligands at free fatty acid receptor 1. J. Biol. Chem. 2009; 284:17527–17539. [PubMed: 19398560]

Song W-J, Jackowski S. Kinetics and regulation of pantothenate kinase from *Escherichia coli*. J. Biol. Chem. 1994; 269:27051–27058. [PubMed: 7929447]

Spry C, van Schalkwyk DA, Strauss E, Saliba KJ. Pantothenate utilization by Plasmodium as a target for antimalarial chemotherapy. Infect. Disord. Drug Targets. 2010; 10:200–216. [PubMed: 20334619]

Sznaidman ML, Haffner CD, Maloney PR, Fivush A, Chao E, Goreham D, Sierra ML, LeGrumelec C, Xu HE, Montana VG, et al. Novel selective small molecule agonists for peroxisome proliferator-activated receptor δ(PPARδ) synthesis and biological activity. Bioorg. Med. Chem. Lett. 2003; 13:1517–1521. [PubMed: 12699745]

Vallee M, Mayo W, Le MM. Role of pregnenolone, dehydroepiandrosterone and their sulfate esters on learning and memory in cognitive aging. Brain Res. Brain Res. Rev. 2001; 37:301–312. [PubMed: 11744095]

Virga KG, Zhang Y-M, Leonardi R, Ivey RA, Hevener K, Park H-W, Jackowski S, Rock CO, Lee RE. Structure-activity relationships and enzyme inhibition of pantothenamide-type pantothenate kinase inhibitors. Bioorg. Med. Chem. 2006; 14:1007–1020. [PubMed: 16213731]

Yun M, Park C-G, Kim J-Y, Rock CO, Jackowski S, Park H-W. Structural basis for the feedback regulation of *Eschericia coli* pantothenate kinase by coenzyme A. J. Biol. Chem. 2000; 275:28093–28099. [PubMed: 10862768]

Zhang JH, Chung TD, Oldenburg KR. A simple statistical parameter for use in evaluation and validation of high throughput screening assays. J. Biomol. Screen. 1999; 4:67–73. [PubMed: 10838414]

Zhang YM, Chohnan S, Virga KG, Stevens RD, Ilkayeva OR, Wenner BR, Bain JR, Newgard CB, Lee RE, Rock CO, Jackowski S. Chemical knockout of pantothenate kinase reveals the metabolic and genetic program responsible for hepatic coenzyme A homeostasis. Chem. Biol. 2007; 14:291–302. [PubMed: 17379144]

Zhang Y-M, Rock CO, Jackowski S. Feedback regulation of murine pantothenate kinase 3 by coenzyme A and coenzyme A thioesters. J. Biol. Chem. 2005; 280:32594–32601. [PubMed: 16040613]

Zhou B, Westaway SK, Levinson B, Johnson MA, Gitschier J, Hayflick SJ. A novel pantothenate kinase gene (*PANK2*) is defective in Hallervorden-Spatz syndrome. Nat. Genet. 2001; 28:345–349. [PubMed: 11479594]

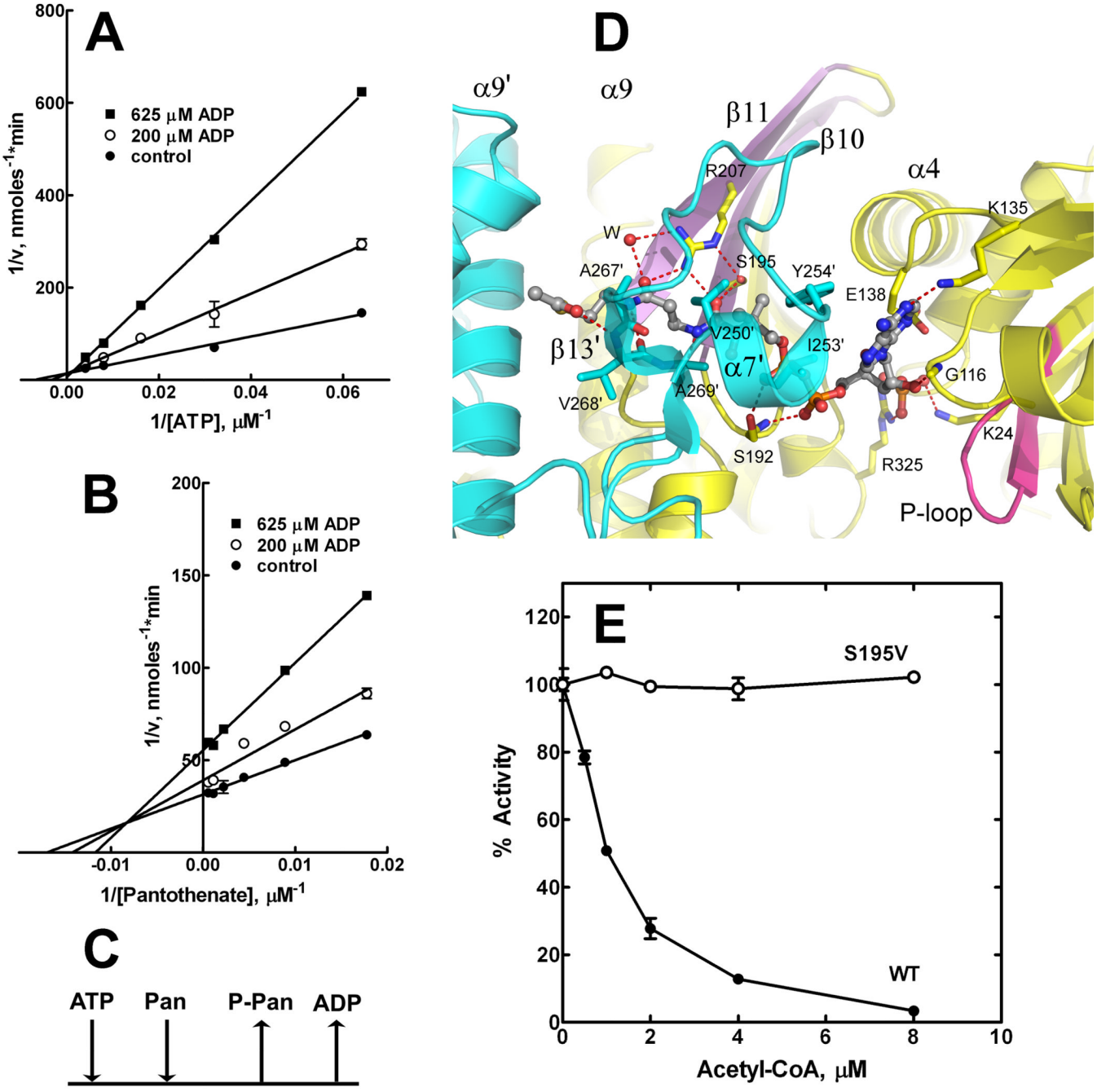

FIGURE 1. Biochemical mechanism and structure of PanK3

Graphical analysis of product inhibition experiments using fixed concentrations of ADP and variable concentrations of either ATP (*A*) or pantothenate (*B*) showed that ADP was competitive with ATP and uncompetitive with pantothenate. (*C*) These data are consistent with a compulsory ordered kinetic mechanism with ATP as the leading substrate and ADP as the last product to leave the enzyme. (*D*) Detailed interactions of the pantothenate portion of CoA within the tunnel formed from the stable β10 and β11 platform of the ATP-binding domain (purple) on one subunit (yellow) and the flexible loop between α7′ and β13′ that reaches over from the opposite monomer (cyan). The residues investigated by site-directed mutagenesis are shown. Acetyl-CoA is shown as a ball-and–stick representation (grey

carbons) and the P-loop is colored magenta. Red spheres are water molecules and hydrogen bonds are indicated by dotted red lines. Note that in this 'open' conformation, the general base E138 is not positioned to perform catalysis and the adenine ring of acetyl-CoA acts as a wedge to prevent domain closure. See Supplementary Experimental Procedures for structure determination and Table 1 for the structural statistics. *(E)* PanK3(S195V) was refractory to acetyl-CoA inhibition compared to PanK3. PanK3 activity in the absence of acetyl-CoA was set at 100%. PanK3(S195V) has a K_M defect for pantothenate (see text). The data were duplicate measurements with the standard error indicated by the bars.

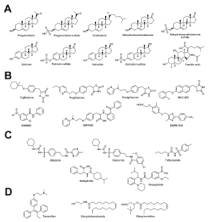

FIGURE 2. Structures of the biochemically characterized inhibitors and activators identified in the HTS

(*A*) Steroids and fusidic acid. (*B*) Thiazolidedione and non-thiazolidinedione PPARγ ligands. (*C*) Sulfonylurea and non sulfonylurea insulin secretagogues. (*D*) PanK3 activators.

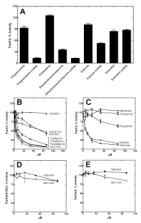

FIGURE 3. PanK3 inhibition by selected compounds identified by HTS

The PanK3 radioactive assay described under “Experimental Procedures” was used to test selected HTS hits and related molecules. (*A*) Steroids and their sulfate derivatives were tested at 100 μM concentration against PanK3. (*B*) The thiazolidinedione PPARγ ligands evaluated were rosiglitazone (●), pioglitazone (○), ciglitazone (■) and MCC-555 (□). Three structurally unrelated PPARγ ligands GW501516 (△), GW1929 (◆) and GW9662 (▲) were also assayed. (*C*) Sulfonylurea insulin secretagogues identified in the HTS, glyburide (●) and glipizide (○) were validated PanK3 inhibitors. Three other insulin secretagogues analyzed were tolbutamide (□), repaglinide (■) and nateglinide (◆). PanK3 activity in the presence of DMSO only was set at 100%. (*D*) PanK3(S195V) was refractory to inhibition by MCC-555 (□) and glyburide (■). (*E*) SaPanK was not inhibited by either MCC-555 (□) or glyburide (■). PanK3 activity in the presence of DMSO only was set at 100%. The specific activities used as 100% in these assays were: PanK3, 149 ± 2 nmoles/min/mg; PanK3(S195V), 48 ± 3 nmoles/min/mg. The data were duplicate measurements with the standard error indicated by the bars. IC_{50} values ± standard error were derived from fitting the 14-point dataset to a single-site binding model using GraphPad software. See Supplementary Fig. S2 for the kinetic analysis of MCC-555 and glyburide inhibition of PanK3 and Supplementary Fig. S3 for the isoform selectivity of MCC-555, glyburide and tamoxifen.

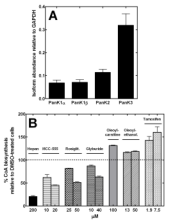

FIGURE 4. The thiazolidinediones inhibit CoA biosynthesis in cell culture

(*A*) Total RNA was extracted from HepG2/C3A cells and real-time PCR was used to determine the relative abundance of the PanK isoform mRNA present normalized to GAPDH as the calibrator. (*B*) HepG2/C3A cells were labeled with [^{3}H]pantothenate and the amount of label incorporated into CoA was determined as described under Experimental Procedures. The amount of incorporation in the control experiment in the presence of DMSO was set at 100%, and the incorporation rates in the presence of the test compounds was expressed as a percent of this value. Hopantenate (Hopan), a known inhibitor of CoA biosynthesis (Zhang et al., 2007) was used as a positive control, MCC-555, rosiglitazone (Rosiglit.), glyburide, oleoyl-carnitine, oleoyl-ethanolaminde and tamoxifen were tested at the indicated concentrations. The data were duplicate measurements with the standard error indicated by the bars.

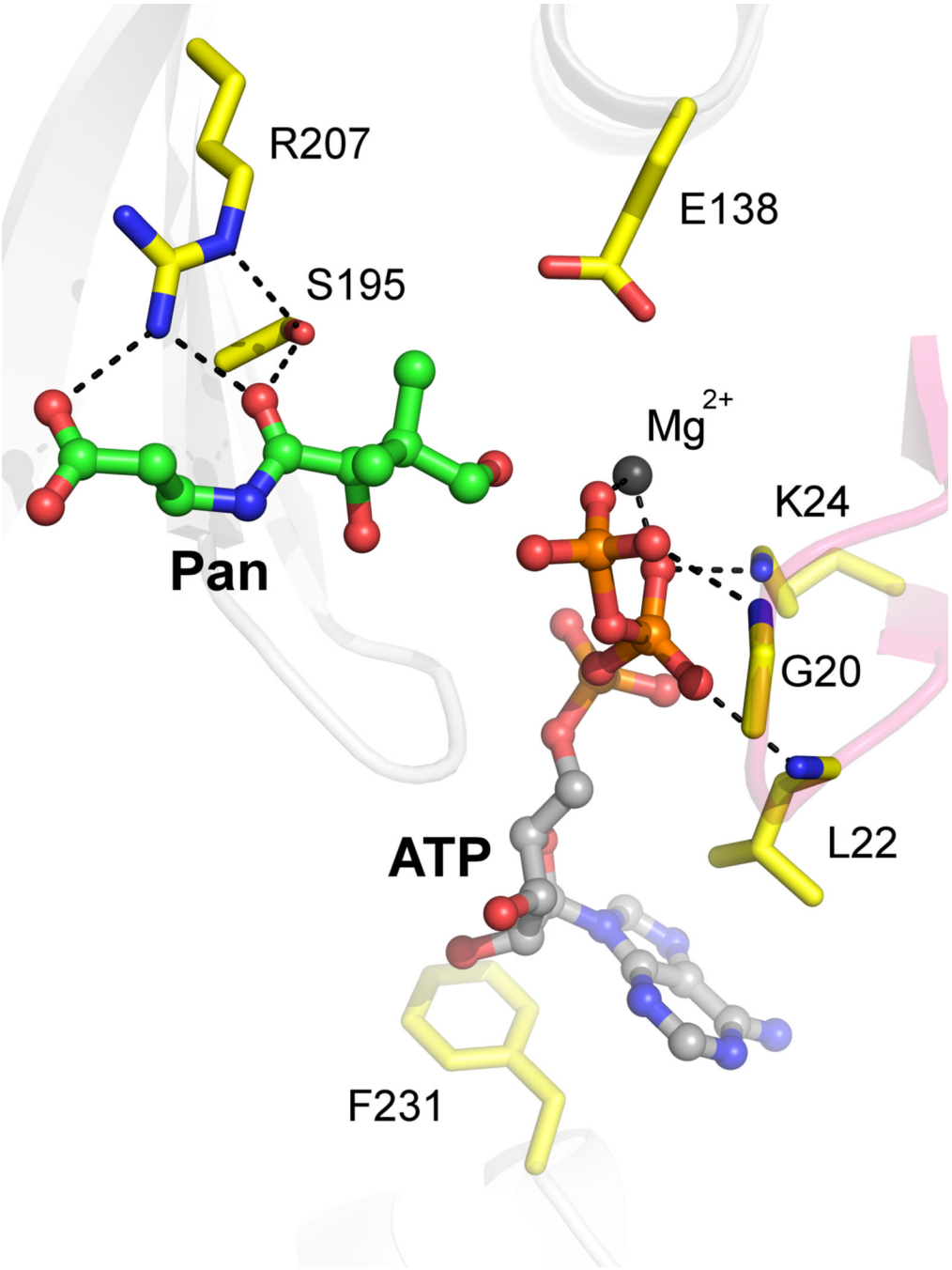

FIGURE 5. Model of the PanK3 'closed' active site

The model is based on the known structure of the homologous *Sa*PanK closed active site. Pantothenate (Pan) carbons are green, protein residues are yellow, Mg^{2+} is a dark grey ball, and ATP carbons are grey. Predicted hydrogen bonds are shown as dashed black lines. The protein backbone is transparent grey, and the P-loop is rendered as transparent magenta. Note that Glu138 is well positioned to act as a general base, unlike the position shown in Fig. 1D. Also, the phosphate groups of ATP engage the P-loop and the adenine ring occupies a pocket that is distinct from that which binds the adenine ring of acetyl-CoA (Fig. 1D).

TABLE 1
Statistics of Data Collection and Refinement

Parameter	PanK3•Acetyl-CoA
Data Collection[a]	
Space group	$P2_1$
Unit cell dimensions (Å)	
a, b, c(Å)	56.7, 180.4, 77.4
α, β, γ(°)	90.0, 95.5, 90.0
Resolution range(Å)	50.0-1.98(2.05-1.98)
Beamline	ID22, SER-CAT
Wavelength(Å)	0.97921
R_{sym}[b]	0.086(0.473)
I/σ	17.5(1.8)
Completeness(%)	98.8(90.2)
Redundancy	3.6(2.7)
Unique reflections	106,621
Refinement [a]	
Resolution range(Å)	50.0-1.98(2.03-1.98)
No. of reflection	100,924(6,914)
Completeness(%)	99.1(92.1)
R_{work}	0.185(0.222)
R_{free}[c]	0.232(0.268)
No. of atoms	
Protein	10,807
Non-protein	775
Mean B overall ($Å^2$)	33
Rmsd from ideal values	
Bond lengths(Å)	0.014
Bond angles(°)	1.462
Ramanchandran plot	
Most favored region(%)	92.6
Additional allowed region(%)	6.9
Generously allowed region(%)	0.4
Disallowed region(%)	0.1

[a] Values in parentheses refer to the highest resolution shell.

[b] $R_{sym} = \Sigma|(I-<I>)|/\Sigma(I)$, where I is the observed intensity.

[c] R_{free} is the R value obtained for a test set of reflections consisting of randomly selected 5% subset of the data set excluded from refinement.

TABLE 2
Bioactive PanK3 inhibitors with an IC_{50} <10 μM

A bioactive compound library of 3,200 unique compounds was initially screened at 12 μM to identify modulators of PanK3 activity. The inhibitors were then individually re-screened using a 10-point concentration series in triplicate, and the IC_{50} values were calculated based on fitting the 30 data points to a single site binding model (see Supplementary Fig. S1). The IC_{50} values were rounded to the nearest 0.1 μM.

Inhibitor	IC_{50} (μM)	Annotated Activity
Fusidic acid	0.1	Antibacterial
1,4-PBIT dihydrobromide	0.4	iNOS and eNOS inhibitor
WIN 62577	0.7	NK1 tachykinin receptor antagonist
Pioglitazone hydrochloride	1.0	Antidiabetic
Reactive Blue 2	1.3	P2Y receptor antagonist
Ephedrine hydrochloride	1.6	Decongestant, bronchodilator
Psi-Rhodomyrtoxin	1.6	Natural product from Rhodomyrtus macrocarpa
Rosiglitazone	1.7	Antidiabetic
Pregnenolone sulfate	2.5	Allosteric modulator of GABA-A receptors
Tyrphostin AG 528	3.0	Protein tyrosin kinase inhibitor
Dehydroisoandrosterone sulfate	3.5	Allosteric modulator of GABA-A receptors
18α-glycyrrhetinic acid	3.6	Anti-inflammatory
Ro 41-0960	3.9	COMT inhibitor
Glipizide	5.2	Antidiabetic
Chloranil	5.9	Antipsoriatic
Glyburide	6.8	Antidiabetic
Hexachlorophene	8.8	Topical anti-infective
Tyrphostin AG 808	9	Protein tyrosine kinase inhibitor
GW5074	9.2	cRaf1 kinase inhibitor
Tolfenamic acid	9.2	Non steroidal anti-inflammatory

TABLE 3
Bioactive PanK3 activators with an EC_{50} <10 μM

A bioactive compound library of 3,200 unique compounds was initially screened at 12 μM to identify modulators of PanK3 activity (HTS). The activators were then individually re-screened using a 10-point concentration series in triplicate. EC_{50} values calculated based on fitting the 30 data points to a single site binding model, and the EC_{50} values were rounded to the nearest 0.1 μM (see Supplementary Fig. S1). The EC_{50} values and the % of maximal activation of PanK3 with respect to the DMSO control were also determined using the PanK3 radioactive assay (RA). See Supplementary Table S1 for the results from the endocannabinoid library screen.

Activator	EC_{50} (μM), HTS[a]	EC_{50} (μM), RA[b]	% Activation RA	Annotated Activity
1,4-naphtoquinone	0.5	Inactive	0	Coal tar product
Phenylmercuric acid[c]	1.0	Inactive	0	Antifungal
Tamoxifen	3.4	4.0	140	Estrogen antagonist
Oleoylethanolamide	7.9	0.5	120	PPARα agonist
Palmitoyl-carnitine	ND[d]	1.6	120	Metabolic intermediate
Oleoyl-carnitine	ND	0.6	140	Metabolic intermediate

[a] High-throughput screening PanK3 assay.

[b] Radiochemical PanK3 assay.

[c] Phenylmercuric acid is an inhibitor of the luciferase reaction accounting for it appearing as a false activator in the HTS.

[d] ND means not determined.